J. Am. Ceram. Soc., 70 [9] 662-68 (1987)

Static Fatigue of Optical Fibers in Bending

M. JOHN MATTHEWSON*,* and CHARLES R. KURKJIAN*

AT&T Bell Laboratories, Murray Hill, New Jersey 07974

A two-point bending technique for making static fatigue measurements on optical fibers is described which allows large quantities of data to be rapidly and conveniently gathered. Statistical analysis is used to compare the times to failure of the method with those of the commonly used mandrel and tensile methods. Direct experimental comparison of the two-point bend and tensile methods shows that while the times to failure are generally longer for two-point bend than tension, the essential fatigue behavior is identical for the two methods.

I. Introduction

STATIC fatigue measurements of lifetime as a function of constant applied stress are widely used to make in-service lifetime predictions but are experimentally inconvenient because of scatter in the failure times. This scatter is typically many times the scatter in the apparent strength, which itself may be large. Even high-strength optical fiber which has a narrow distribution of strength may have over 50% scatter in the time to failure, and a minimum of 20 specimens is needed for each applied stress to produce statistically reliable results. A further inconvenience is that failure times should be made as long as possible to optimize the reliability of extrapolations to longer-term in-service conditions. Clearly, making long-time measurements on many specimens is an onerous task requiring large amounts of time and equipment. We describe here a two-point bending technique for optical fibers which tests many specimens simultaneously and, since it is compact, enables many sets of specimens to be packed into an environmental chamber alleviating the long-duration problem. The advantages and disadvantages of the technique will be discussed and a detailed comparison will be made with the other two techniques that are commonly used, namely tension and mandrel bending.

Presented in part at the 87th Annual Meeting of the American Ceramic Society, Cincinnati, OH, May 6, 1985 (Glass Division, Paper No. 14-G-85). Received December 22, 1986; revised copy received April 3, 1987; approved April 14, 1987.

*Member, the American Ceramic Society.

*Present address: IBM Almaden Research Center, San Jose, CA 95120-6099.

II. Apparatus

Figure 1 is a schematic diagram of the apparatus used for the three techniques under discussion.

In the tensile technique, described in detail by Krause,[1] a length of fiber is gripped at each end and pulled in tension using weights. It is usually inconvenient to immerse the grips in the test environment and therefore the fiber is threaded through an environmental chamber. If bare fiber is to be studied, the polymeric protective coating applied during manufacture may be stripped from the center section by immersion in 200°C concentrated sulfuric acid. However, the coating must be intact at the grips and where it passes through seals into the environmental chamber to avoid mechanical damage at these locations.

The mandrel bending technique involves winding a length of fiber around a precision-ground mandrel. The fiber must be coated by a protective polymer layer to avoid damage from contact with the mandrel and adjacent windings. The bending stress is determined by the mandrel radius and the entire mandrel is placed in the environment to be studied. Holding the ends of the fiber in place is a major drawback with this technique; mechanically gripping the ends or gluing them in place produces stress concentrations which cause premature failure. Tape may be wrapped around the ends but it must be chosen carefully since the adhesive can provide an aggressive environment which again leads to premature failure. Bouten and Wagemans[2] described an ingenious modification in which the fiber is wound around two adjacent mandrels of differing radii. Gluing onto the larger radius mandrel produces stress concentrations which are insignificant compared with the stress generated in the fiber section passing around the smaller mandrel. Bouten and Wagemans applied a glue line along the entire length of the fiber winding so that each turn of fiber is a small but separate specimen and a statistically reliable lifetime estimate can be made from one winding. However, whatever gripping technique is used it must be significantly more resistant to the test environment than

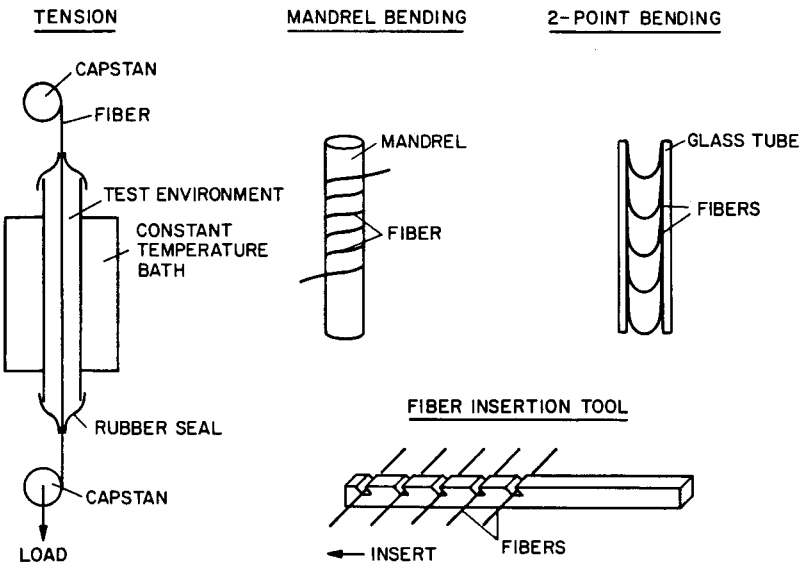

Fig. 1. Schematic diagram of the apparatus used by the three techniques for static fatigue testing of optical fiber. Also shown is the insertion tool for inserting several specimens into a tube simultaneously.

the fiber itself and this is difficult to realize in practice for the aggressive environment used in accelerated testing.

The two-point bend technique, first described by Cowap and Brown,[3] involves bending a short length of fiber double and inserting it into a precision-bore glass tube. Many specimens may be inserted into one tube and the stress applied to them is determined by the tube internal diameter. Several specimens may be inserted at once using the insertion tool shown in Fig. 1. Because the "teeth" are inclined, the tool may be withdrawn from the tube without disturbing the fiber loops.

Fracture of the fibers is monitored acoustically. The transducer output is passed through a trigger circuit which emits a pulse whenever the output exceeds a certain level. The pulses may be monitored by a chart recorder, though a computer is more convenient in more rapid experiments where the short interval between pulses requires better frequency response. The chart recorders represent the most expensive part of the apparatus, but the required number of channels can be simply halved. If the output of two trigger circuits are subtracted and applied to one recorder channel, pulses from one circuit produce positive going pulses on the chart while the other produces negative going pulses. In this way each recorder channel can monitor two separate experiments. Coated fiber must be inserted into the tube to avoid mechanical damage but the properties of bare fiber can be investigated by stripping the fiber in situ by sucking hot sulfuric acid into the tube or by immersing the tube in a bath of acid. Coated fibers may be placed in the tube as close as 2 mm apart without interaction but bare fibers should be at least 10 mm apart and the bend should point downward so that debris from fractured fiber falls onto the compressive side of the adjacent fibers.

The two-point bend technique has features which may in some applications make it more useful than the tensile or mandrel techniques, or both:

(1) Many specimens are handled and tested at once. It is as convenient to test several in two-point bend, giving a reliable time-to-failure estimate, as it is to test just one specimen using the other techniques. Thus although the actual time to failure in blending is somewhat longer, the total time, and in particular the "operator" time, may be substantially less.

(2) There are no gripping problems in two-point bend.

(3) The tube is compact and, once inserted, the fibers are protected from accidental damage. It is therefore simple to apply a test environment either by immersion or by passing fluid through a tube.

(4) Small quantities of fiber are used—an advantage if supplies are limited.

(5) The behavior of both coated and bare fiber can be examined. Bare fibers cannot be used in mandrel bending. If bare fiber is examined in tension, coated regions must be preserved for gripping and passing through environmental seals. Difficulties arise if the bare section is stronger than the coated section; fracture in the bare section can be assured by necking it down, but in general the properties of the fiber will be changed by heating to the softening temperature.

(6) Static fatigue in two-point bend directly corresponds with the dynamic strength test in bending described in detail by Matthewson, Kurkjian, and Gulati.[4] There is no dynamic strength test corresponding to mandrel bending.

(7) The stress distribution experienced by the fiber in two-point bend directly corresponds to the practical situation where a fiber cable is bent around a corner.

(8) The technique is compact, inexpensive, and easy to use. Only a small amount of equipment is needed to monitor several hundred specimens under test simultaneously.

There are, however, some characteristics of two-point bending that may make it an inappropriate technique in certain situations:

(1) The tested length of fiber is small and two-point bend results are not useful for predicting the behavior of kilometer lengths of fiber. However, this is also true of mandrel bending and tension unless multikilometer lengths of fiber are tested.

(2) Because of the stochastic nature of strength, the mean lifetime of a fiber depends on its length. It is not possible to control the length of fiber under test as it just depends on the tube diameter.

(3) The mean lifetime depends on the tested length of specimen but the tested length depends on the tube bore size (i.e., the applied stress) which itself affects the lifetime. This effect needs to be understood before results can be compared with other methods.

(4) The times to failure for two-point bend are longer than those for the other methods because of the shorter tested length. However, the increased duration of experiments is more than compensated by the ability to test many specimens simultaneously.

(5) The technique is not suitable under conditions where significant fatigue occurs during specimen mounting and preparation and environmental equilibration. This effectively limits the applied stress to less than 3 GPa for coated fiber and to 2 GPa for fiber stripped in hot acid while in the tube. The minimum time to failure is limited to the time it takes the specimen to equilibrate with the test environment. This problem can be avoided by mounting specimens under low stress in the dynamic bend apparatus[4] and loading rapidly to the required applied stress after equilibration with the test environment. However, only a few specimens can be tested at once and one of the main advantages of the two-point technique is lost.

(6) Bare fibers cannot be inserted into the tubes without damage. The fatigue properties of bare fiber that has been treated in some way under zero stress cannot be determined with this technique.

The first four disadvantages concern the effect of specimen size on the time to failure. In order to fully understand this, the effective tested length must be calculated and its effect on the statistics of failure must be understood.

III. Statistical Analysis of Fatigue

The statistical nature of the fiber lifetime results from two sources; first, from the stochastic nature of strength which is determined by strength-reducing surface defects that are distributed in severity and position, and second, from diameter fluctuations along the length of the fiber. Generally one or other of these sources will dominate and determine the statistics. For example, Kurkjian and Paek[5] found that all variation in apparent strength of high-strength furnace-drawn silica fibers could be accounted for by diameter fluctuations and that variation in real strength was insignificant. Conversely, the properties of a fiber showing a broad strength distribution, which in the case of optical fiber is virtually any fiber but high-quality as-drawn material, will be determined by the distribution of defects. Both sources of lifetime variations will now be considered.

(1) Statistics of Strength Variation

In order to develop a statistical analysis it is necessary to know how the time to failure depends on the applied stress and also on the distribution of initial strengths. Neither behavior is known a priori but reasonable relationships may be chosen and justified empirically.

First, we will consider fibers containing flaws that behave like small cracks. The well-known power-law relationship between the crack growth velocity, $\dot{c}$, and the applied stress intensity factor, K_I, has been found to hold empirically for a wide range of ceramics:

$$\dot{c} = AK_I^n \tag{1}$$

where A depends on the environment, and n, the stress corrosion susceptibility parameter, is roughly independent of the environment and is often considered a material property. This equation may be integrated by using the fracture mechanics relation

$$K_I = Y\sigma_a c^{1/2} \tag{2}$$

to give the time to failure

$$t_f = \frac{2}{n-2}\frac{1}{AY^2}\frac{1}{K_{IC}^{n-2}}\frac{\sigma_i^{n-2}}{\sigma_a^n} \tag{3}$$

where Y is a factor of order unity dependent on the crack geometry, K_{IC} is the critical stress intensity factor, σ_i is the initial strength, and σ_a is the applied stress (e.g., Ritter[6]).

High-strength silica fibers do not contain well-defined cracklike defects; if this were the case, cracks would be of atomic dimensions and could not be described by continuum fracture mechanics. The n value for bulk silica is around 40 as measured from both crack growth experiments (e.g., Sakaguchi, Sawaki, Abe, and Kawasaki[7]) and fatigue experiments (e.g., Ritter and Sherburne[8]). This compares with the accepted value of between 20 and 25 for fibers (e.g., Wang and Zupko[9]). Recent work by Dabbs and Lawn[10] sheds light on the nature of the high-strength defects. They find an n of 40 for "postthreshold" microindention flaws, after correction for residual stresses, and an n of 20 for "subthreshold" flaws. These latter flaws represent strengths in excess of 300 MPa and are not associated with the presence of cracks.

Empirically, a power-law relationship between t_f and σ_a is observed for fibers and we may assume

$$t_f = B\frac{\sigma_i^p}{\sigma_a^n} \tag{4}$$

where $p = n - 2$ for cracklike flaws but for noncracklike flaws p is not known, but will not differ significantly from $n - 2$ since if c now represents some measure of flaw severity we might expect Eq. (1) to still hold empirically. Equation (2) will not necessarily hold but since its effect is to provide the "2" in the terms "$n - 2$" in Eq. (3), the difference between p and $n - 2$ will be small as $n \gg 2$. The analysis will be developed for general p, but p will be evaluated as $n - 2$ in all calculations.

The two-parameter Weibull distribution for the initial strength will be assumed, giving the cumulative probability of failure by a stress σ in the absence of fatigue:

$$F(\sigma, A) = 1 - \exp\left[-\left(\frac{\sigma}{\sigma_0}\right)^m \frac{A}{A_0}\right] \tag{5}$$

where A is the specimen surface area and A_0 is a parameter of dimension area and size unity which gives σ_0 the dimensions of stress. For an element of area, dA, the probability becomes

$$dF(\sigma, dA) = \left(\frac{\sigma}{\sigma_0}\right)^m \frac{dA}{A_0} \tag{6}$$

Rearranging Eq. (4) gives

$$\sigma_i = \left(\frac{t_f \sigma_a^n}{B}\right)^{1/p} \tag{7}$$

and failure occurs in the absence of fatigue if $\sigma_i < \sigma$. Therefore, in the presence of fatigue, the probability that failure occurs by a time t_f is obtained by substituting the expression for σ_i in Eq. (7) for σ in Eq. (6).

$$dF(t_f, dA) = \left(\frac{t_f \sigma_a^n}{B\sigma_0^p}\right)^{m/p} \frac{dA}{A_0} \tag{8}$$

Integration of the applied stress, σ_a, over the entire specimen surface gives the cumulative failure probability

$$F(t_f, A) = 1 - \exp\left[-\int \left(\frac{t_f \sigma_a^n}{B\sigma_0^p}\right)^{m/p} \frac{dA}{A_0}\right]$$

$$= 1 - \exp\left[-\int f(t_f, \sigma_a)\frac{dA}{A_0}\right] \tag{9}$$

This integration will now be evaluated for the three test methods under discussion.

(*A*) *Uniaxial Tension:* For the tensile test σ_a is a constant and the integration of Eq. (9) gives

$$\int f(t_f, \sigma_a)\, dA = \left(\frac{t_f \sigma_a^n}{B\sigma_0^p}\right)^{m/p} \frac{2\pi r l_t}{A_0} \tag{10}$$

where r and l_t are the fiber radius and tensile test length.

By comparison with Eq. (5) we see that the failure time follows a Weibull distribution with modulus

$$m_t = m/p \tag{11}$$

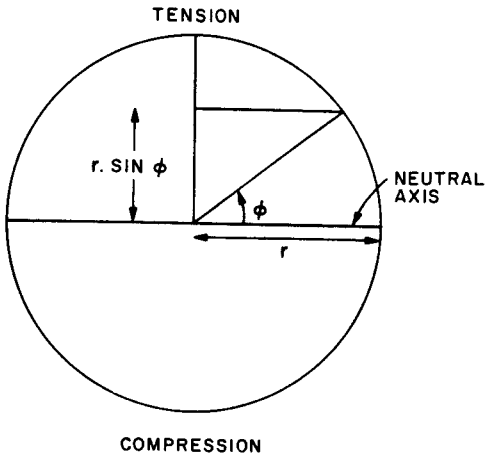

Fig. 2. Section through the bent fiber.

and a mean failure time

$$\bar{t}_t = \frac{B\sigma_0^p}{\sigma_a^n}\left(\frac{A_0}{2\pi r l_t}\right)^{1/m_t} \Gamma(1 + 1/m_t) \tag{12}$$

where $\Gamma(x)$ is the gamma (or factorial) function which may be evaluated from polynomial approximations (e.g., Hastings[11]).

(*B*) *Mandrel Bending:* In mandrel bending the fiber experiences a uniform bend along its length. The surface tensile stress varies around the fiber circumference (Fig. 2)

$$\sigma_a(\phi) = \sigma_{max} \sin \phi$$

where σ_{max} is the maximum tensile stress in the fiber surface.

$$\sigma_{max} = E\frac{r}{R + r'}$$

where R is the mandrel radius, r' is the fiber radius including the coating material, and E is the fiber Young's modulus. A suitable surface area element is

$$dA = l_m r\, d\phi$$

where l_m is the length of fiber wrapped around the mandrel. Integration of Eq. (9) over the tensile half of the specimen surface gives

$$\int f(t_f, \sigma_a)\, dA = \left(\frac{t_f \sigma_{max}^n}{B\sigma_0^p}\right)^{m/p} \frac{2rl_m}{A_0} I\left(\frac{nm}{p}\right) \tag{13}$$

where

$$I(x) = \int_0^{\pi/2} \sin^x \zeta\, d\zeta = \frac{\pi^{1/2}}{2} \frac{\Gamma\left(\frac{x+1}{2}\right)}{\Gamma\left(\frac{x}{2} + 1\right)}$$

Equation (13) represents a Weibull distribution again with

$$m_t = m/p$$

and a mean time to failure

$$\bar{t}_m = \frac{B\sigma_0^p}{\sigma_{max}^n}\left[\frac{A_0}{2rl_m I(nm_t)}\right]^{1/m_t} \Gamma(1 + 1/m_t) \tag{14}$$

(*C*) *Two-Point Bending:* The analysis for the two-point bend, described in Matthewson, Kurkjian, and Gulati,[4] gives

$$\sigma_a(\theta, \phi) = \sigma_{max} \sin^{1/2} \theta \sin \phi$$

(see Fig. 3) where σ_{max} is the maximum stress in the fiber surface

$$\sigma_{max} = 1.198E\frac{2r}{d - 2r'}$$

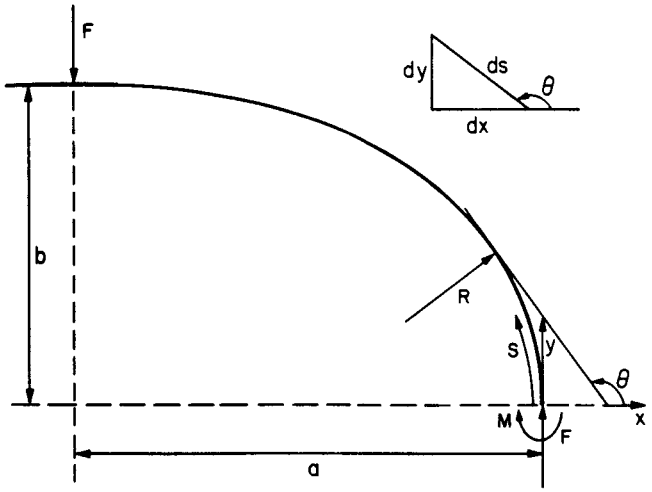

Fig. 3. Geometry of the bent fiber in two-point bending.

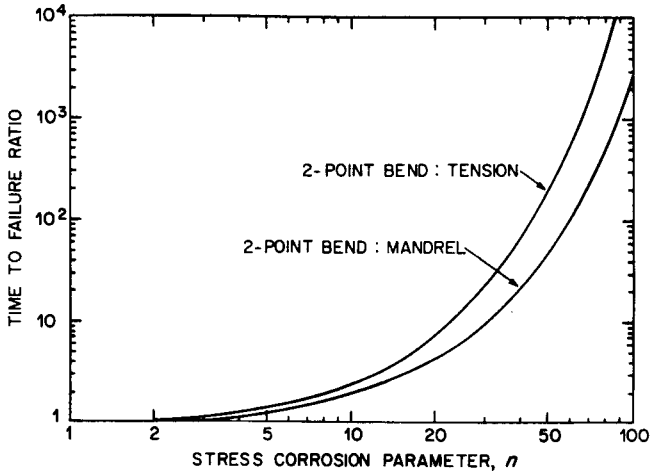

Fig. 4. Variation of the time-to-failure ratios with n for two-point bend compared to tension and mandrel bending.

and d is the internal tube diameter. A suitable area element is

$$dA = \frac{Er^2}{\sigma_{max} \sin^{1/2} \theta} d\theta \, d\phi$$

Equation (9) gives

$$\int f(t_f, \sigma_a) \, dA = \left(\frac{t_f \sigma_{max}^n}{B\sigma_{max}}\right)^{m/p} \frac{4Er^2}{A_0 \sigma_{max}} I\left(\frac{nm - p}{2p}\right) I\left(\frac{nm}{p}\right) \tag{15}$$

Again a Weibull distribution with

$$m_t = m/p$$

and a mean time to failure

$$\bar{t}_2 = \frac{B\sigma_0^p}{\sigma_{max}^n}\left[\frac{A_0 \sigma_{max}}{4Er^2 I\left(\frac{nm_t - 1}{2}\right) I(nm_t)}\right]^{1/m_t} \Gamma(1 + 1/m_t) \tag{16}$$

All three test methods give Weibull distributions for the times to failure with the same exponent, $m_t = m/p$. For cracklike flaws $m_t = m/(n - 2)$, which is in agreement with the results of an analysis for tensile testing by Key, Fox, and Fuchs.[12] The mean times to failure are related to the applied stress (σ_a for tension and σ_{max} for bending) by a power law giving an effective stress corrosion parameter, n_{eff}, of n for tension and mandrel bending and $n(1 - p/nm)$ for two-point bend, which is little different from n for large n.

The mean times to failure will now be examined in more detail.

(*D*) *Time-to-Failure Ratios:* From Eqs. (16) and (12) the ratio of the time to failure in two-point bend and tension is given by equating σ_a to σ_{max}:

$$\frac{\bar{t}_2}{t_t} = \left[\frac{\sigma_{max}}{E} \frac{l_t}{r} \frac{\pi}{2I\left(\frac{nm_t - 1}{2}\right) I(nm_t)}\right]^{1/m_t} \tag{17}$$

and depends on the applied strain, the tensile specimen aspect ratio, and a function of n, p, and m. The ratio of failure times for two-point bend and mandrel bending from Eqs. (16) and (14) is

$$\frac{\bar{t}_2}{t_m} = \left[\frac{\sigma_{max}}{E} \frac{l_m}{r} \frac{1}{2I\left(\frac{nm_t - 1}{2}\right)}\right]^{1/m_t} \tag{18}$$

Figure 4 shows the variation of the time-to-failure ratios, Eqs. (17) and (18), with the stress corrosion parameter, n. The results are calculated for 1-m-long tensile and mandrel fibers of diameter 125 μm with an applied strain of 5%. It is assumed that the Weibull modulus of the distribution of inert strengths is 100 and $p = n - 2$. For a typical silica fiber of $n = 20$, the times to failure in two-point bending are approximately 7 and 4 times longer than those for the tensile and mandrel tests. These factors increase rapidly with increasing n.

(*E*) *Equivalent Tensile Length:* The equivalent tensile length will now be calculated for each bend method. This is the length of fiber that, when pulled in tension, gives the same time to failure as a bend specimen subjected to the same stress.

Equations (14) and (12) give the time-to-failure ratios for mandrel bending and tension

$$\frac{\bar{t}_m}{t_t} = \left[\frac{l_t}{l_m} \frac{\pi}{I(nm_t)}\right]^{1/m_t} \tag{19}$$

and when this ratio is equated to unity, the equivalent tensile length is

$$l_{t,m} = l_m \frac{I(nm_t)}{\pi} \tag{20}$$

Equating the ratio to unity in Eq. (17) gives the equivalent length for two-point bending

$$l_{t,2} = r \frac{E}{\sigma_{max}} \frac{2I\left(\frac{nm_t - 1}{2}\right) I(nm_t)}{\pi} \tag{21}$$

Figure 5 shows the variation of the equivalent lengths, given by Eqs. (20) and (21), with stress corrosion parameter, n, calculated using the same parameter values as Fig. 4. For values of n above about 10 the equivalent length is roughly constant at ~17 mm for two-point bending and 40 μm for a 1-m-length mandrel bend specimen. Therefore, all three methods test quite different effective specimen sizes.

(2) *Statistics of Fiber Diameter Variation*

The scatter in the fiber diameter results in a scatter in the applied stress when the fiber is under load. If the scatter in the fiber strength is insignificant, the fiber will fail at the minimum or maximum diameter (depending on the test method) and the diameter fluctuations must be characterized before predictions from apparent strength statistics can be made. However, the nature of the diameter fluctuations, which depend on the fiber draw parameters, are not easily predicted and vary from fiber to fiber. Krawarik and Watkins[13] examined diameter distributions of early fibers and found their spectra were similar to low-pass filtered white noise with little evidence of periodic fluctuations. The diameter distributions could be approximated by the Gaussian function with a standard deviation of ~1 μm. However, improvements in diameter

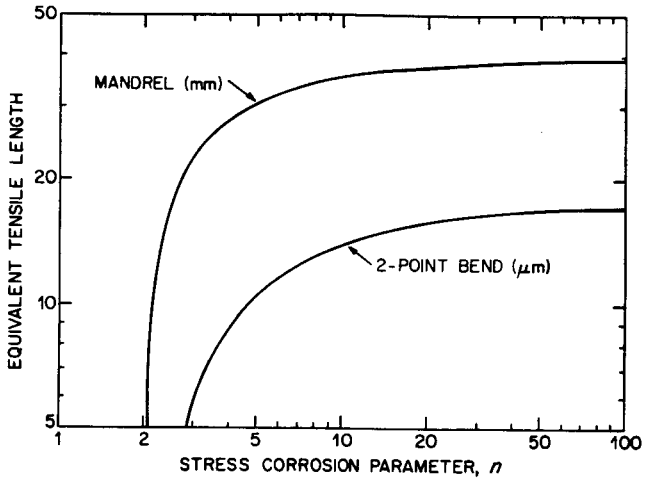

Fig. 5. Variation of the equivalent tensile length with n for two-point and mandrel bending.

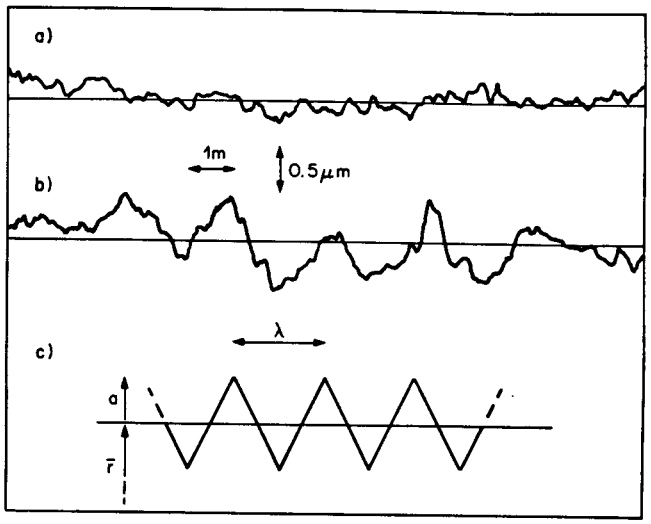

Fig. 6. Radius fluctuations (a and b) of a typical optical fiber and (c) idealized periodic fluctuation.

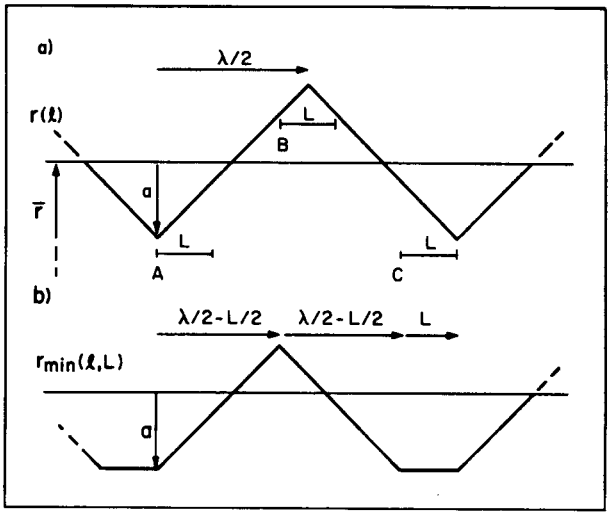

Fig. 7. Periodic fiber radius fluctuations: (a) radius as a function of position, (b) minimum radius over a length L as a function of position along the fiber.

control equipment now have reduced the deviation to ~0.25 μm.

Figure 6 shows continuous measurements of fiber diameter taken during the drawing process for 125-μm-diameter silica optical fiber and Fig. 6(a) shows a region in which the fluctuations are random and have a broad-band noise spectrum and are probably due to intrinsic properties of the silica, such as local viscosity fluctuations that occur when the fiber is molten in the draw furnace.

The fiber diameter is controlled in the drawing process by monitoring it at some distance, D say, from the draw furnace. The output from the diameter transducer is used as a feedback signal to control the draw tension which in turn controls the diameter. Since the position of the diameter transducer is spatially separated from the neckdown zone in the draw furnace, it is possible to set up periodic diameter oscillations if the properties of the feedback loop are not carefully chosen and such oscillations are apparent in Fig. 6(b) and approximate the triangular waveform of Fig. 6(c). This fiber was drawn at unusually low speed to aid resolving short-length diameter fluctuations and the feedback parameters were not optimal. In the absence of damping the oscillations would have a half-wavelength equal to D but damping in the feedback loop increases this wavelength so that the measured value of $\lambda \simeq 2m$ is consistent with $D \simeq 0.5m$.

Specimens of length greater than the wavelength will contain at least one diameter minimum and will fail there in tension and the apparent strength statistics will depend on the random distribution of the values of the minima. In contrast, specimens shorter than λ do not necessarily contain a diameter minimum and so will sample the complete diameter range. Provided random fluctuations are much smaller than a, the amplitude of periodic fluctuations, averaging for several specimens will tend to remove them, giving results which are characteristic of the underlying periodic variation. Therefore, the statistics of long and short (compared to λ) specimens would be of a different nature and depend on different quantities. They will not correlate in general and it is therefore not possible to infer the properties of long specimens from those of short if periodic fluctuations dominate.

(*A*) *Periodic Diameter Fluctuations:* We will first consider only the periodic fluctuations and assume that the random fluctuations are of smaller amplitude so that they average out over several specimens. Figure 7(a) models the radius as a triangular waveform of wavelength λ and peak aplitude a. A triangular wave is chosen for mathematical simplicity but the analysis can be extended to describe any waveform. Figure 7(b) shows the minimum radius on a specimen of length L as a function of its position, l, along the fiber and is given by

$$r_{min}(l, L) = a\left(\frac{4l}{\lambda} - 1\right) + \bar{r} \qquad \left(0 \le l \le \frac{\lambda - L}{2}\right)$$

$$= a\left(3 - \frac{4L}{\lambda} - \frac{4l}{\lambda}\right) + \bar{r} \qquad \left(\frac{\lambda - L}{2} \le l \le \lambda - L\right)$$

$$= \bar{r} - a \qquad (\lambda - L \le l \le \lambda)$$

giving a mean value

$$\bar{r}_{min} = \bar{r}\left[1 - \frac{a}{\bar{r}}\frac{L}{\lambda}(2 - L/\lambda)\right] = \bar{r}(1 - \delta) \tag{22}$$

For a typical silica optical fiber $a = 0.5$ μm and $\bar{r} = 62.5$ μm so that δ ranges from 0 for $L = 0$ and 1/125 for $L \ge \lambda$. However, measurements of both strength[4] and fatigue (see Section IV) in tension ($L \simeq \lambda$) and bending ($L/\lambda \ll 1$) give results that differ by significantly more than is permitted by Eq. (22). Hence, the effect of random diameter fluctuations dominates over periodic fluctuations observed in this fiber.

(*B*) *Random Diameter Fluctuations:* In tensile experiments the load, P, is conserved along the fiber. The nominal (σ_{nom}) and ac-

tual applied stresses (σ_a) at any position on the fiber are given by

$$\sigma_{nom} = \frac{P}{\pi \bar{r}^2}; \quad \sigma_a = \frac{P}{\pi r^2}$$

$$\sigma_a = \sigma_{nom} \frac{\bar{r}^2}{r^2} \quad \text{(tension)} \tag{23}$$

In mandrel bending the radius of curvature, R, of the fiber is constrained to be constant

$$\sigma_{nom} = E\frac{\bar{r}}{R}; \quad \sigma_a = E\frac{r}{R}$$

$$\sigma_a = \sigma_{nom} \frac{r}{\bar{r}} \quad \text{(mandrel bend)} \tag{24}$$

For two-point bend, the bending moment M_b is conserved

$$EI/R = M_b$$

where I is the second moment of sectional area and depends on r^4, hence

$$\sigma_a = \sigma_{nom} \frac{\bar{r}^4}{r^4} \quad \text{(two-point bend)} \tag{25}$$

Equations (23), (24), and (25) imply that failure occurs at the position of minimum radius in tension and two-point bend but at the position of maximum radius in mandrel bending. Therefore, a Weibull distribution cannot be used to describe radius fluctuations for all three cases as it cannot be modified to simultaneously describe the statistics of the minimum and maximum radii since the minimum radius in a length l diverges as l becomes very small; the maximum radius is therefore unbounded for this distribution. Other suitable distributions could be used, such as the normal distribution, but the mathematics would rapidly become intractable and for this reason the statistical analysis of radius fluctuations will not be considered further.

IV. Experimental Procedure

Figure 8 directly compares static fatigue results obtained using both two-point bend and tension techniques. A standard 125-μm silica optical fiber coated with a UV-curable polyurethane-acrylate protective coating was used and the test environment was 90°C distilled water. Attempts to obtain data using mandrel bending were unsuccessful since no adhesive system could be found for fixing fiber ends that could withstand this aggressive environment for more than an hour or so.

Sixty bend and ten tensile specimens were used for each data point and, despite the considerably larger number of bend specimens and their longer time to failure, it took appreciably less time to obtain all the bend data. Error bars representing the confidence in the estimate of the mean time to failure are typically of the size of the plotted data points or smaller and are omitted.

The two sets of data show identical behavior and are merely shifted in time from one another. From 10^2 to 10^5 s linear fatigue is observed with a slope giving a value for the stress corrosion parameter, n, of between 40 and 50. Above $\sim 10^5$ s, n again increases, suggesting perhaps either a fatigue limit or a return to its previous higher value. At times to failure of less than ~ 10 s the bend results show an upward turn which is an artifact — the specimens do not have time to equilibrate with their environment on this time scale. This fatigue behavior is complex and will not be discussed in detail here. Suffice to say that we have attributed the change in slope of n going from ~ 50 to ~ 1 to an exaggeration of the change (20 to 7) observed for uncoated fiber in hot water (Krause[1]) and the coated fiber in high humidity (Wang and Zupko[9]).

The two-point bend data are represented analytically in Fig. 8 by cubic splines (solid line) from which the predicted tensile behavior (dashed line) is calculated using Eq. (17) and using the tensile test length, $l_t = 0.18$ m and assuming $m = 100$ and $p = n - 2$. The agreement between the tensile data and the predictions is only

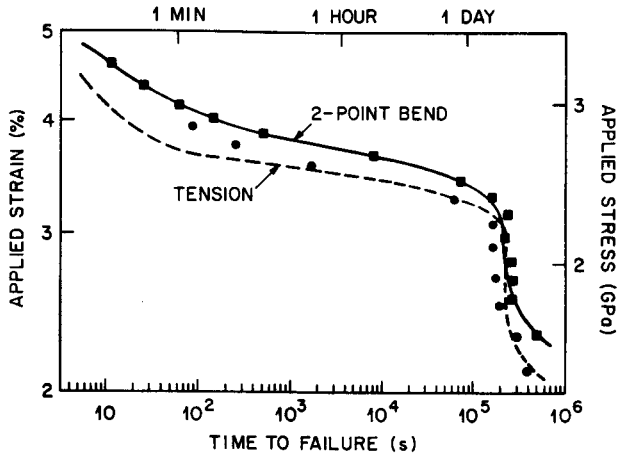

Fig. 8. Direct comparison of fatigue data using the tension (circles) and two-point bending (squares) techniques for polymer-coated optical fiber in 90°C water.

moderate as might be expected, first, because the fatigue is nonlinear, but more importantly the statistical nature of the failure times is due to scatter in the fiber diameter, rather than in the fiber strength, as is assumed in deriving Eq. (17). While it is not possible to infer tensile results from bend data or *vice versa*, the important point to note from Fig. 8 is that bending and tension show the same form for the environmental behavior. In other experiments using a variety of environments we have not observed any significant differences between the bending and tensile fatigue behavior. We may therefore conclude that both techniques are observing the same physical processes.

The variability in the times to failure for this fiber, at least initially, is due to fluctuations in the applied stress caused by diameter variability. The gradient of the log (applied stress) *versus* log (time to failure) curve is identified with the local value of $-1/n$ from Eq. (4):

$$\frac{d(\log \sigma_a)}{d(\log t_f)} = -\frac{1}{n} \tag{26}$$

giving

$$\frac{d\sigma_a}{\sigma_a} \Big/ \frac{dt_f}{t_f} = -\frac{1}{n} \tag{27}$$

so that

$$\nu_t = n\nu_\sigma \tag{28}$$

where ν_t and ν_σ are the dispersions (defined as the ratio of standard deviation to mean) for the time to failure and applied stress. High-strength fibers typically have a Weibull modulus of $m \simeq 100$, giving a value of ν_σ of 1.27%. Figure 9 shows the predicted behavior of the dispersion in the time to failure calculated by obtaining the variation of n by differentiating the spline representation of the fatigue data in Fig. 8. Also shown are experimentally determined values for dispersion with error bars representing 95% confidence intervals on the mean. There is close agreement between experiment and predictions at all but the smaller dispersions where extraneous experimental errors contribute to the variability; there is therefore internal consistency in the data. The value n may be calculated either from the dispersion or from the fatigue curve; however, the latter method gives a value of n averaged over an interval of time while the former gives the local value. For example, an applied strain of 3.3% gives a mean time to failure of 80 000 s with a dispersion of 30%. In the absence of longer-term data, a "by-eye" examination of Fig. 8 would lead one to the erroneous conclusion that the fatigue curve can be extrapolated to longer time/lower stress with of high value of $n \simeq 50$. However, the dispersion is too low to support this conclusion and

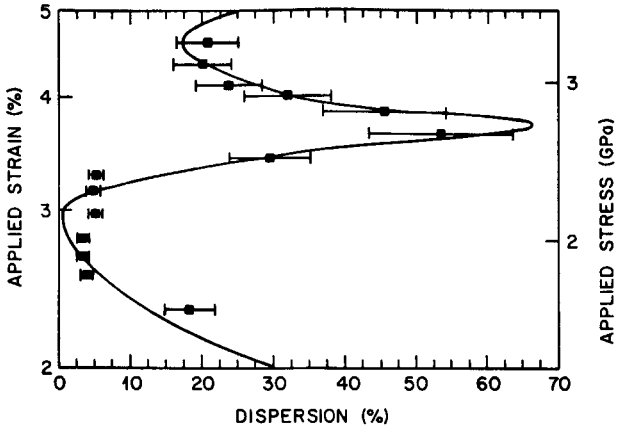

Fig. 9. Experiment and predicted behavior for the dispersion in the times to failure.

gives warning of the abrupt change of fatigue behavior at longer times/lower stresses.

While Kurkjian and Paek[5] showed that diameter variation dominates for short-term strength measurements, it does not necessarily follow that this should be the case for long-term fatigue experiments. In fact, the rather drastic changes in dispersion shown in Fig. 9 may well signal changes in mechanism. However, it is probably safe to assume that the flaws subjected to the largest stress intensity factor lead to failure in both cases. Whether diameter fluctuations dominate or not though, dispersion measurements will not detect the difference since, if fatigue were controlled by strength fluctuations

$$\nu_t \simeq p\nu_\sigma \tag{29}$$

from Eq. (1) and the fact that the dispersion of a Weibull distribution is approximately inversely proportional to the modulus. p and n differ by a small amount and Eqs. (28) and (29) are indistinguishable within the experimental uncertainty.

V. Discussion and Conclusions

The two-point bend method for the static fatigue of optical fibers has been shown to be a useful technique that readily produces large amounts of data. It is a particularly useful method for aggressive test environments which would make gripping the fiber a problem for other techniques. The experimental apparatus is inexpensive and compact, so that the technique is particularly suitable for long-term testing of large numbers of specimens under simulated operating conditions, as well as under accelerated laboratory conditions.

A very small amount of fiber is under stress in the two-point bend test and, because the statistical distributions of fiber strength and diameter are not known a priori, it is not possible to predict tensile behavior from bend behavior. However, since one is concerned in practice with multikilometer lengths, neither 1-m tensile specimens nor bend test specimen can be used to infer multikilometer statistics. This is not only because of the large difference in lengths, but also because the natures of the strength-determining flaws in long fiber lengths are often different and can sometimes be associated with extrinsic effects such as particulate contamination of the silica surface during the drawing process. These types of defects may well show different fatigue behavior, though the "subthreshold" flaws of Dabbs and Lawn,[10] which may model them, do show the same value for n as high-strength fiber, so that all types of flaws may well fatigue in a similar manner.

Experiments have shown that while two-point bending results are different from the tensile results, the form of the fatigue behavior is identical. Bending has been shown to produce internally consistent data in the sense that dispersion in the time to failure is consistent with the overall fatigue behavior. Also, because bending can easily produce much data, statistically significant estimates of dispersion can be obtained which supply extra information.

Acknowledgments: We thank J. T. Krause for useful discussions and R. C. Huff for providing the fiber diameter data.

References

[1]J. T. Krause, "Zero Stress Strength Reduction and Transitions in Static Fatigue of Fused Silica Fiber Lightguides," *J. Non-Cryst. Solids*, **38–39**, 497–502 (1980).
[2]P. C. P. Bouten and H. H. M. Wagemans, "Double Mandrel: A Modified Technique for Studying Static Fatigue of Optical Fibers," *Electron. Lett.*, **20** [7] 280–81 (1984).
[3]S. F. Cowap and S. D. Brown, "Static Fatigue Testing of a Hermetically Sealed Optical Fiber," *Am. Ceram. Soc. Bull.*, **63** [3] 495 (1984).
[4]M. J. Matthewson, C. R. Kurkjian, and S. T. Gulati, "Strength Measurement of Optical Fibers by Bending," *J. Am. Ceram. Soc.*, **69** [11] 815–21 (1986).
[5]C. R. Kurkjian and U. C. Paek, "Single-Valued Strength of "Perfect" Silica Fibers," *Appl. Phys. Lett.*, **42** [3] 251–53 (1983).
[6]J. E. Ritter, Jr., "Probability of Fatigue Failure in Glass Fibers," *Fiber Integr. Opt.*, **1**[4] 387–99 (1978).
[7]S. Sakaguchi, Y. Sawaki, Y. Abe, and T. Kawasaki, "Delayed Failure in Silica Glass," *J. Mater. Sci.*, **17**, 2878–86 (1982).
[8]J. E. Ritter, Jr., and C. L. Sherburne, "Dynamic and Static Fatigue of Silicate Glasses," *J. Am. Ceram. Soc.*, **54** [12] 601–605 (1971).
[9]T. T. Wang and H. M. Zupko, "Long-Term Mechanical Behaviour of Optical Fibres Coated with a UV-Curable Epoxy Acrylate," *J. Mater. Sci.*, **13**, 2241–48 (1978).
[10]T. P. Dabbs and B. R. Lawn, "Strength and Fatigue Properties of Optical Glass Fibers Containing Microindentation Flaws," *J. Am. Ceram. Soc.*, **68** [11] 563–69 (1985).
[11]C. Hastings, Jr., Approximations for Digital Computers. Princeton University Press, Princeton, NJ, 1955.
[12]P. L. Key, A. Fox, and E. O. Fuchs, "Mechanical Reliability of Optical Fibers," *J. Non-Cryst. Solids*, **38–39**, 463–68 (1980).
[13]P. H. Krawarik and L. S. Watkins, "Fiber Geometry Specifications and Its Relation to Measured Fiber Statistics," *Appl. Opt.* **17**, 3984–89 (1978). □